SO(10) SUSY GUT for fermion masses: Lepton flavor and *CP* violation

R. Dermíšek,[1] M. Harada,[2] and S. Raby[2]

[1]*School of Natural Sciences, Institute for Advanced Study, Princeton, New Jersey 08540, USA*

[2]*Department of Physics, The Ohio State University, 191 W. Woodruff Avenue, Columbus, Ohio 43210, USA*

(Received 8 June 2006; published 28 August 2006)

We discuss the results of a global χ^2 analysis of a simple $SO(10)$ supersymmetric grand unified theory (SUSY GUT) with D_3 family symmetry and low energy R parity. The model describes fermion mass matrices with 14 parameters and gives excellent fits to 20 observable masses and mixing angles in both quark and lepton sectors, giving six predictions. Bi-large neutrino mixing is obtained with hierarchical quark and lepton Yukawa matrices, thus avoiding the possibility of large lepton flavor violation. The model naturally predicts small 1–3 neutrino mixing, with $\sin\theta_{13} \simeq 0.05$–$0.06$. In this paper we evaluate the predictions for the lepton flavor violating processes, $\mu \to e\gamma$, $\tau \to \mu\gamma$ and $\tau \to e\gamma$ and also the electric dipole moment of the electron (d_e), the muon, and the tau, assuming universal squark and slepton masses (m_{16}) and a universal soft SUSY breaking A parameter (A_0) at the GUT scale. We find $\mathrm{Br}(\mu \to e\gamma)$ is naturally below present bounds, but may be observable by MEG. Similarly, d_e is below present bounds, but it is within the range of future experiments. We also give predictions for the light Higgs mass (using FEYNHIGGS). We find an upper bound given by $m_h \leq 127$ GeV, with an estimated ± 3 GeV theoretical uncertainty. Finally we present predictions for SUSY particle masses in the favored region of parameter space.

DOI: 10.1103/PhysRevD.74.035011 PACS numbers: 12.10.Dm, 12.60.Jv, 14.60.Pq

I. INTRODUCTION

In this paper we present results for a global χ^2 analysis of the $SO(10)$ supersymmetric grand unified theory (SUSY GUT) for fermion masses presented in Ref. [1]. The model also has a $D_3 \times [U(1) \times Z_2 \times Z_3]$ family symmetry.[1] The three families of quarks and leptons are contained in three 16 dimensional representations of $SO(10)$ $\{16_a, 16_3\}$ with 16_a ($a = 1, 2$) a D_3 flavor doublet (see Ref. [2] for details on D_3). The third family, along with the pair of electroweak Higgs doublets, contained in the 10 dimensional representation of $SO(10)$, consists of D_3 singlets. Hence only the third generation has a renormalizable Yukawa coupling and, as a consequence, we have $\lambda_t = \lambda_b = \lambda_\tau = \lambda_{\nu_\tau}$ Yukawa unification at M_{GUT}. This forces us into the large $\tan\beta$ regime and several interesting predictions follow. We have derived the consequences of third generation Yukawa unification in several papers. In Ref. [4] we demonstrated that in order to fit the low energy values of the top, bottom and tau masses (with the typically large, of order 50%, radiative corrections to the bottom quark mass) the soft SUSY breaking parameters necessarily reside in a very narrow region of the possible parameter space. Hence we have definite predictions for SUSY spectra; see [4] and Sec. IV for more details. In addition, in this region of parameter space the light Higgs mass necessarily has a central value of order 120 GeV. In Ref. [5] we demonstrated that this same minimal $SO(10)$ SUSY model ($\mathrm{MSO_{10}SM}$) gives the correct abundance of dark matter, fitting the WMAP data, and gives observable values for the branching ratio $\mathrm{Br}(B_s \to \mu^+\mu^-)$ with a lower bound of order 10^{-8}. The dark matter candidate in this model is the lightest supersymmetric particle (LSP), neutralino, which predominantly annihilates through a direct s-channel CP-odd Higgs, A. In addition, it also dominates in the leptonic decay of B_s.

In the present model, all of the above results are retained (with small modifications), but in addition we fit the masses and mixing angles of all three families, including neutrino data. The model describes fermion mass matrices with 14 parameters and gives excellent fits to 20 observable masses and mixing angles in both quark and lepton sectors, giving six predictions. Both the charged fermion and neutrino mass matrices are hierarchical, thus suppressing large flavor violating interactions, even at large $\tan\beta$. The simple structure of the neutrino sector leads quite naturally to maximal atmospheric neutrino oscillations and large solar neutrino mixing [1]. We predict a very small value for $\sin\theta_{13} \simeq 0.05$–$0.06$. In addition, CP violation in the neutrino sector is fixed by the phases in the charged fermion mass matrices. At the same time we can easily accommodate leptogenesis via nonthermal processes; see for example [6].

II. THE MODEL

The full superpotential $W = W_{\mathrm{ch.fermions}} + W_{\mathrm{neutrino}}$ for fermion masses and mixing angles contains two terms. The first term, resulting in Dirac Yukawa matrices for charged fermions and neutrinos, is given by

$$W_{\mathrm{ch.\ fermions}} = 16_3 10 16_3 + 16_a 10 \chi_a + \bar{\chi}_a \Big(M_\chi \chi_a + 45 \frac{\phi_a}{\hat{M}} 16_3 + 45 \frac{\tilde{\phi}_a}{\hat{M}} 16_a + \mathbf{A} 16_a \Big). \quad (1)$$

[1]The charged fermion sector of this theory was considered in an earlier paper [2] and the neutrino sector of the theory was inspired by the previous analysis by one of us, R.D. [3].

The third family of quarks and leptons is contained in the superfield 16_3 [transforming as a 16 of $SO(10)$]; the first two families are contained in 16_a ($a = 1, 2$) [with explicit $SO(10)$ transformations and transforming as a D_3 doublet) and the two Higgs doublets are contained in 10. The additional fields are an adjoint of $SO(10)$ (45) and several $SO(10)$ singlet flavon fields needed to break the full flavor symmetry $D_3 \times [U(1) \times Z_2 \times Z_3]$. Note that $M_\chi = M_0(1 + \alpha X + \beta Y)$ includes $SO(10)$ breaking vacuum expectation values (VEVs) in the X and Y directions; ϕ^a, $\tilde{\phi}^a$ (D_3 doublets), $\mathbf{A}$ ($\mathbf{1_B}$ singlet) are $SO(10)$ singlet flavon fields, and $\hat{M}$, M_0 are $SO(10)$ singlet masses. The fields 45, $\mathbf{A}$, ϕ, $\tilde{\phi}$ are assumed to obtain VEVs $\langle 45 \rangle \sim (B - L)M_G$ (where B, L, M_G are baryon and lepton number and the GUT scale, respectively), $\mathbf{A} \ll M_0$, and

$$\langle \phi \rangle = \begin{pmatrix} \phi_1 \\ \phi_2 \end{pmatrix}, \qquad \langle \tilde{\phi} \rangle = \begin{pmatrix} 0 \\ \tilde{\phi}_2 \end{pmatrix} \tag{2}$$

with $\phi_1 > \phi_2$. The second term gives large lepton number violating masses for ''right-handed'' neutrinos, necessary for the seesaw mechanism. We have

$$\begin{aligned} W_{\text{neutrino}} = \overline{16}(\lambda_2 N_a 16_a + \lambda_3 N_3 16_3) \\ + \tfrac{1}{2}(S_a N_a N_a + S_3 N_3 N_3) \end{aligned} \tag{3}$$

where the fields N_3, N_a ($a = 1, 2$) are $SO(10)$ singlets and $\overline{16}$ is assumed to break $SO(10)$ to $SU(5)$ via a VEV in the right-handed neutrino direction.

The superpotential [Eq. (1)] results in the following Yukawa matrices[2]:

$$\begin{aligned} Y_u &= \begin{pmatrix} 0 & \epsilon'\rho & -\epsilon\xi \\ -\epsilon'\rho & \tilde{\epsilon}\rho & -\epsilon \\ \epsilon\xi & \epsilon & 1 \end{pmatrix}\lambda, \\ Y_d &= \begin{pmatrix} 0 & \epsilon' & -\epsilon\xi\sigma \\ -\epsilon' & \tilde{\epsilon} & -\epsilon\sigma \\ \epsilon\xi & \epsilon & 1 \end{pmatrix}\lambda, \end{aligned} \tag{4}$$

$$\begin{aligned} Y_e &= \begin{pmatrix} 0 & -\epsilon' & 3\epsilon\xi \\ \epsilon' & 3\tilde{\epsilon} & 3\epsilon \\ -3\epsilon\xi\sigma & -3\epsilon\sigma & 1 \end{pmatrix}\lambda, \\ Y_\nu &= \begin{pmatrix} 0 & -\epsilon'\omega & \frac{3}{2}\epsilon\xi\omega \\ \epsilon'\omega & 3\tilde{\epsilon}\omega & \frac{3}{2}\epsilon\omega \\ -3\epsilon\xi\sigma & -3\epsilon\sigma & 1 \end{pmatrix}\lambda, \end{aligned} \tag{5}$$

with

$$\begin{gathered} \xi = \phi_2/\phi_1, \qquad \tilde{\epsilon} \propto \tilde{\phi}_2/\hat{M}, \qquad \epsilon \propto \phi_1/\hat{M}, \\ \epsilon' \sim (\mathbf{A}/M_0), \qquad \sigma = \frac{1+\alpha}{1-3\alpha}, \qquad \rho \sim \beta \ll \alpha, \\ \omega = 2\sigma/(2\sigma - 1). \end{gathered} \tag{6}$$

The Dirac mass matrices are then given by

$$m_i \equiv Y_i \frac{v}{\sqrt{2}} \sin\beta, \qquad i = \nu, u, \tag{7}$$

$$m_i \equiv Y_i \frac{v}{\sqrt{2}} \cos\beta, \qquad i = e, d. \tag{8}$$

Consider the neutrino masses. In the three 16's we have three electroweak doublet neutrinos (ν_a, ν_3) and three electroweak singlet antineutrinos ($\bar{\nu}_a$, $\bar{\nu}_3$). In addition, the antineutrinos get GUT scale masses by mixing with three $SO(10)$ singlets $\{N_a, a = 1, 2; N_3\}$ transforming as a D_3 doublet and singlet, respectively. We assume $\overline{16}$ obtains a VEV, v_{16}, in the right-handed neutrino direction, and $\langle S_a \rangle = M_a$ for $a = 1, 2$ (with $M_2 > M_1$) and $\langle S_3 \rangle = M_3$.[3] We thus obtain the effective neutrino mass terms given by

$$W = \nu m_\nu \bar{\nu} + \bar{\nu} V N + \tfrac{1}{2} N M_N N \tag{9}$$

with

$$V = v_{16}\begin{pmatrix} 0 & \lambda_2 & 0 \\ \lambda_2 & 0 & 0 \\ 0 & 0 & \lambda_3 \end{pmatrix}, \qquad M_N = \text{diag}(M_1, M_2, M_3). \tag{10}$$

The electroweak singlet neutrinos $\{\bar{\nu}, N\}$ have large masses $V, M_N \sim M_G$. After integrating out these heavy neutrinos, we obtain the light neutrino mass matrix given by

$$\mathcal{M} = m_\nu M_R^{-1} m_\nu^T, \tag{11}$$

where the effective right-handed neutrino Majorana mass matrix is given by

$$M_R = V M_N^{-1} V^T \equiv \text{diag}(M_{R_1}, M_{R_2}, M_{R_3}), \tag{12}$$

with

$$\begin{gathered} M_{R_1} = (\lambda_2 v_{16})^2/M_2, \qquad M_{R_2} = (\lambda_2 v_{16})^2/M_1, \\ M_{R_3} = (\lambda_3 v_{16})^2/M_3. \end{gathered} \tag{13}$$

Defining U_e as the 3×3 unitary matrix for left-handed leptons needed to diagonalize Y_e [Eq. (4)], i.e. $Y_e^D = U_e^T Y_e U_{\tilde{e}}^*$ and also U_ν such that $U_\nu^T \mathcal{M} U_\nu = \mathcal{M}_D = \text{diag}(m_{\nu_1}, m_{\nu_2}, m_{\nu_3})$, then the neutrino mixing matrix is given by $U_{\text{PMNS}} = U_e^\dagger U_\nu$ in terms of the flavor eigenstate (ν_α, $\alpha = e, \mu, \tau$) and mass eigenstate (ν_i, $i = 1, 2, 3$) basis

[2] In our notation, Yukawa matrices couple electroweak doublets on the left to singlets on the right. It has been shown in Ref. [7] that excellent fits to charged fermion masses and mixing angles are obtained with this Yukawa structure.

[3] These are the most general set of VEVs for ϕ_a and S_a. The zero VEV for $\tilde{\phi}_1$ can be enforced with a simple superpotential term such as $S\tilde{\phi}_a\tilde{\phi}_a$.

fields with

$$\nu_\alpha = \sum_i (U_{\rm PMNS})_{\alpha i} \nu_i. \tag{14}$$

For $U_{\rm PMNS}$ we use the notation of Ref [8] with

$$\begin{pmatrix} \nu_e \\ \nu_\mu \\ \nu_\tau \end{pmatrix} = \begin{pmatrix} c_{12}c_{13} & s_{12}c_{13} & s_{13}e^{-i\delta} \\ -s_{12}c_{23} - c_{12}s_{23}s_{13}e^{i\delta} & c_{12}c_{23} - s_{12}s_{23}s_{13}e^{i\delta} & s_{23}c_{13} \\ s_{12}s_{23} - c_{12}c_{23}s_{13}e^{i\delta} & -c_{12}s_{23} - s_{12}c_{23}s_{13}e^{i\delta} & c_{23}c_{13} \end{pmatrix} \begin{pmatrix} e^{i\alpha_1/2}\nu_1 \\ e^{i\alpha_2/2}\nu_2 \\ \nu_3 \end{pmatrix}. \tag{15}$$

Finally, we note that this theory is certainly not fundamental with many arbitrary symmetry breaking VEVs at the GUT scale. Nevertheless, it has two major features in its favor. As a result of the GUT and family symmetries, the Yukawa matrices, which are the only observables of the complicated GUT physics, have fewer parameters than low energy observables. Hence this theory is predictive. Second, the model has the advantage that it self-consistently fits the low energy data, and thus, at the very least, it is an excellent phenomenological ansatz for fermion masses. Thus it can be tested via additional low energy flavor violating processes.

III. GLOBAL χ^2 ANALYSIS

Yukawa matrices in this model are described by seven real parameters $\{\lambda, \epsilon, \tilde{\epsilon}, \sigma, \rho, \epsilon', \xi\}$ and, in general, four phases $\{\Phi_\sigma, \Phi_{\tilde{\epsilon}}, \Phi_\rho, \Phi_\xi\}$. Therefore, in the charged fermion sector we have 11 parameters to explain nine masses and three mixing angles and one CP violating phase in the Cabibbo-Kobayashi-Maskawa (CKM) matrix, leaving us with two predictions.[4] Note that these parameters also determine the neutrino Yukawa matrix. Finally, our minimal ansatz for the right-handed neutrino mass matrix is given in terms of three additional real parameters,[5] i.e. the three right-handed neutrino masses. At this point the three light neutrino masses and the neutrino mixing matrix, $U_{\rm PMNS}$ ($3 + 4$ observables), are completely specified. Altogether, the model describes 20 observables in the quark and lepton sectors with 14 parameters, effectively having six predictions.[6]

In addition to the parameters describing the fermion mass matrices, we have to input three parameters specifying the three gauge couplings: the GUT scale M_G defined as the scale at which α_1 and α_2 unify, the gauge coupling at the GUT scale α_G, and the correction ϵ_3 to $\alpha_3(M_G)$ necessary to fit the low energy value of the strong coupling constant. Finally we have to input seven supersymmetry parameters given by the following: $M_{1/2}$, a universal gaugino mass; m_{10}, a universal Higgs mass; m_{16}, a universal squark and slepton mass; A_0, a universal trilinear coupling; a small Higgs mass splitting parameter, $\Delta m_H = 1/2(m^2_{H_d} - m^2_{H_u})/m^2_{10}$; the supersymmetric Higgs mass parameter $\mu(M_Z)$; and the ratio of the two Higgs VEVs, $\tan\beta$.

We have also imposed some physically motivated constraints on the χ^2 analysis. We demand a lower bound on the lightest stop mass given by $m_{\tilde{t}} = 500$ GeV. Lower values of $m_{\tilde{t}}$ actually give even better fits. On the other hand, a chargino-stop loop gives the dominant SUSY contribution to the process $b \to s\gamma$ and lighter stop values make it difficult to fit this process. In addition we fix the CP-odd Higgs mass, $m_A = 700$ GeV. Lower values would result in a branching ratio $\mathrm{Br}(B_s \to \mu^+\mu^-)$ which approaches the experimental lower bound; see Ref. [5]. Our results, however, are not sensitive to this latter constraint. Further discussion of the former constraint is given in Sec. IV.

All the parameters [except for $\mu(M_Z)$] are run from the GUT scale to the weak scale (M_Z) using two-loop (one-loop) renormalization group equations, or RGEs, for dimensionless (dimensionful) parameters. At the weak scale, the SUSY partners are integrated out leaving the two Higgs doublet model as an effective theory. We require proper electroweak symmetry breaking. Moreover, the full set of one-loop electroweak and SUSY threshold corrections to fermion mass matrices, as well as to the three precision electroweak observables [G_μ, α^{-1}_{EM}, and $\alpha_s(M_Z)$], are calculated at M_Z.[7] Below M_Z

[4]Of course, in any supersymmetric theory there is one additional parameter in the fermion mass matrices, i.e. $\tan\beta$. Including this parameter, there is one less prediction for fermion masses, but then (once SUSY is discovered) we have one more prediction. This is why we have not included it explicitly in the preceding discussion.

[5]In principle, these parameters can be complex. We will nevertheless assume that they are real; hence there are no additional CP violating phases in the neutrino sector.

[6]Note that the two Majorana phases are, in principle, observable, for example, in neutrinoless double-beta decay [9]; however, the measurement would be very difficult (perhaps too difficult [10]). If observable, this would increase the number of predictions to eight.

[7]In a top down analysis, the $\overline{DR}$ value of $\sin^2\theta_W(M_Z)$ is obtained directly via RG running $\alpha_{(1,2)}$ from the GUT scale. Then, with the calculated value of M_Z and all one-loop threshold corrections included in Δr, we obtain the observed value of G_μ [11].

we use three-loop QCD and one-loop QED RG equations to calculate light fermion masses and $\alpha_{\rm EM}$. More details about the analysis can be found in [4] or [5].[8] In addition, we self-consistently include the contributions of the right-handed neutrinos to the RG running between the GUT scale and the mass of the heaviest right-handed neutrino [12].

The χ^2 function is constructed from observables given in Table II. We have used the top quark mass from the PDG reviews of particle properties 2005 update by T. M. Liss and A. Quadt.[9] Note that we have included several redundant observables in the quark sector. We do this because quark masses are not known with high accuracy and different combinations of quark masses usually have independent experimental and theoretical uncertainties. Thus we include three observables for the charm and bottom quark masses: the $\overline{\rm MS}$ running masses $[m_c(m_c), m_b(m_b)]$ and the difference in pole masses $M_b - M_c$ obtained from heavy quark effective theory. The same is true for observables in the CKM matrix. For example, we include V_{td} and the two CP violating observables ϵ_K and the value for $\sin(2\beta)$ given by the world average measured via the process $B \to J/\psi K_s$ [14]. However, we have doubled the error to take into account the significant difference between the *BABAR* and Belle central values. We thus have 16 observables in the quark and charged lepton sectors. We use the central experimental values and one-sigma error bars from the Particle Data Group [8]. However, in the case that the experimental error is less than 0.1%, we use $\sigma = 0.1\%$ due to the numerical precision of our calculation.

At present only four observables in the neutrino sector are measured. These are the two neutrino mass squared differences, Δm^2_{31} and Δm^2_{21}, and two mixing angles, $\sin^2\theta_{12}$ and $\sin^2\theta_{23}$. For these observables we use the central values and 2σ errors from Ref. [15]. The other observables—neutrino masses, 1–3 mixing angles, and the phase of the lepton mixing matrix—are predictions of the model. In addition, the new feature of this paper is the predictions for several lepton flavor violating (LFV) processes and lepton electric dipole moments (EDMs).

IV. RESULTS

Let us now discuss our results. We performed the global χ^2 analysis for values of the soft SUSY breaking scalar mass at M_G given by $m_{16} = 3$, 4, and 5 TeV. However, we only present the results for the latter two cases. Good fits prefer the region of SUSY parameter space characterized by[10]

$$\mu, M_{1/2} \ll m_{16}, \qquad -A_0 \simeq \sqrt{2} m_{10} \simeq 2 m_{16}. \tag{16}$$

This is required in order to fit the top, bottom, and tau masses when the third generation Yukawa couplings unify [4]. Note that the three input parameters $(\mu, M_{1/2}, m_{16})$ are not varied when minimizing χ^2. As a consequence of the relations [Eq. (16)], we expect heavy first and second generation squarks and sleptons, while the third generation scalars are significantly lighter (with the stop generically the lightest). In addition, charginos and neutralinos are typically the lightest superpartners. We predict values of $\tan\beta \sim 50$ and a light Higgs with mass $m_h \leq 127$ GeV (with a theoretical uncertainty ± 3 GeV). The specific relations between the SUSY breaking parameters also lead to an interesting prediction for the process $B_s \to \mu^+\mu^-$ with a branching ratio in the region currently being explored at the Tevatron.[11] Furthermore, the neutralino relic density obtained for our best fit parameters is consistent with WMAP data [5] and direct neutralino detection is possible in near-future experiments. Finally, this region maximally suppresses the dimension five contribution to proton decay [16] and suppresses SUSY flavor and CP violation in general. For more information on the SUSY and Higgs spectra and related phenomenology in this region of SUSY breaking parameter space, see Refs. [4,5].

In Figs. 1 and 2 we present contours of constant χ^2 for $m_{16} = 4$ and 5 TeV with $m_A = 700$ GeV, as a function of μ, $M_{1/2}$. The best fits are obtained for small values of $M_{1/2} \leq 300$ GeV (where the lower bound on $M_{1/2}$ is determined by the experimental bound on the chargino mass, $m_{\chi^+} > 104$ GeV). We find that the value of χ^2 decreases as m_{16} increases. This is solely due to the lower bound of 500 GeV on the lightest stop mass and the resultant difficulty in fitting the bottom quark mass with a heavier stop.

At this point, a brief aside is necessary. In our analysis, we have not evaluated several significant pieces of data. These include the branching ratios $\mathrm{Br}(b \to s\gamma)$ and $\mathrm{Br}(B \to X_s l^+ l^-)$, and $B_s - \bar{B}_s$ mixing. These also provide significant constraints on the theory. However, we have used the code of T. Blažek [7,17] to check our analysis and also evaluate the branching ratio $\mathrm{Br}(b \to s\gamma)$. This process is enhanced at large $\tan\beta$. The dominant SUSY contribution comes from the chargino-stop loop. We find that the most significant constraint is a lower bound on the lightest

[8]The only difference is that in the present analysis we include all three families of fermions.

[9]This value of the top quark mass (172.7 ± 2.9 GeV/c^2) is not so different from the most recent value ($172.5 \pm 1.3_{\rm stat} \pm 1.9_{\rm syst}$GeV/c^2) from CDF II and DZero at the Tevatron [13].

[10]In addition, the best fit requires a nonuniversal Higgs mass at the GUT scale with $\Delta m_H = 1/2(m^2_{H_d} - m^2_{H_u})/m^2_{10} \sim 0.07$. Note that this is significantly smaller than needed in the past [4]. That is because the RGE running of neutrino Yukawas from M_G to the heaviest right-handed neutrino has been included self-consistently. As noted in [4], such running was a possible source for Higgs splitting. Evidently it cannot be the only source.

[11]This process is sensitive to the CP-odd Higgs mass, m_A, which can be adjusted in theories with nonuniversal Higgs masses.

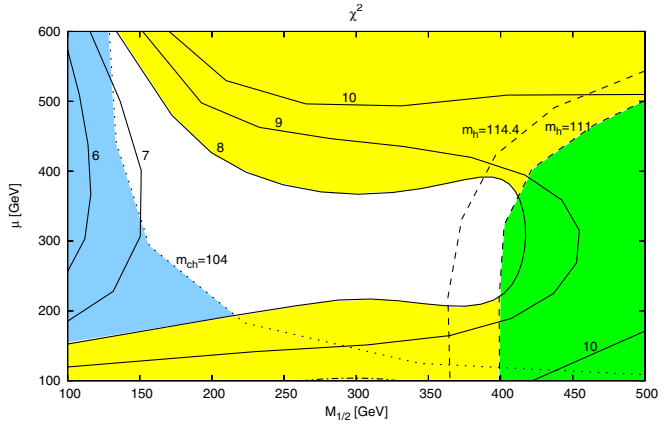

FIG. 1 (color online). Contours of constant χ^2 for $m_{16} = 4$ TeV and $m_A = 700$ GeV. The yellow (very light) shaded region at the bottom and top (and the region bounded by the extended solid boundary line) has $\chi^2 \geq 8$. The blue (light shaded) region on the left (and below the extended dotted line) is excluded by $m_{\chi^+} < 104$ GeV and the green (darker shaded) region is excluded by the Higgs mass bound $m_h < 111$ GeV.

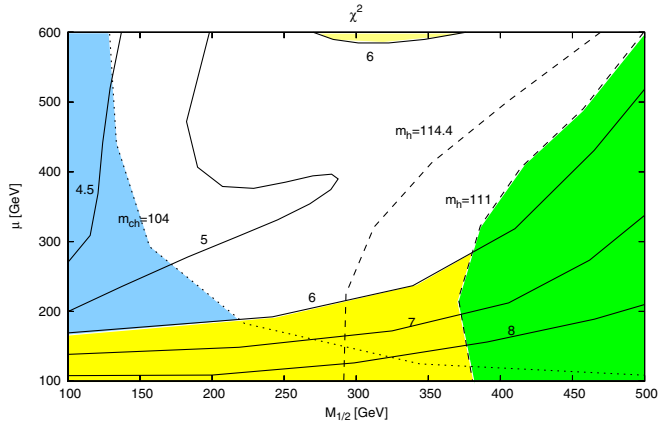

FIG. 2 (color online). Contours of constant χ^2 for $m_{16} = 5$ TeV and $m_A = 700$ GeV. The yellow (very light) shaded region at the bottom and top (and the region bounded by the extended boundary line) has $\chi^2 \geq 6$. The blue (light shaded) region on the left (and below the extended dotted line) is excluded by $m_{\chi^+} < 104$ GeV and the green (darker shaded) region is excluded by the Higgs mass bound $m_h < 111$ GeV.

stop mass of order 500 GeV. We have thus imposed this bound on the stop mass by introducing a penalty to χ^2. The best fit for the branching ratio $\mathrm{Br}(b \to s\gamma)$ is then fit with the minimal stop mass. Note, we find that χ^2 increases as the lower bound on the stop mass increases. This is due to the fact that a good fit for m_b prefers a light stop [4,5]. In addition, as the lower bound on the stop mass increases, we find it necessary to increase m_{16}. For example, with the light stop mass, $m_{\tilde{t}} = 300$ GeV, we find good fits with $m_{16} = 3$ TeV [4]. Now with $m_{\tilde{t}} = 500$ GeV, good fits, with $\chi^2 \leq 8$, are only obtained with $m_{16} \geq 4$ TeV. As a

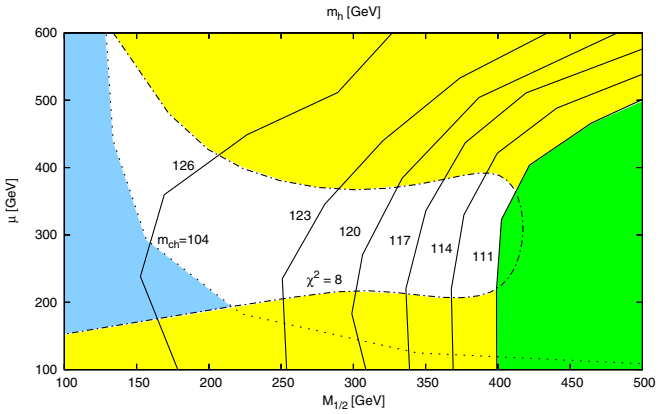

FIG. 3 (color online). Contours of constant light Higgs mass m_h for $m_{16} = 4$ TeV and $m_A = 700$ GeV. The shaded regions are the same as in Fig. 1.

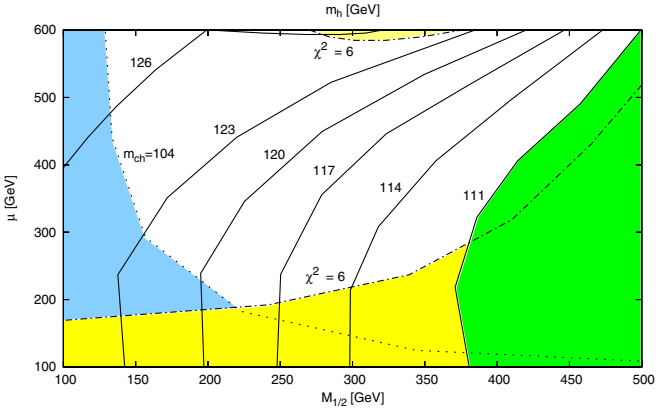

FIG. 4 (color online). Contours of constant light Higgs mass m_h for $m_{16} = 5$ TeV and $m_A = 700$ GeV. The shaded regions are the same as in Fig. 2.

final note, for a light stop ($m_{\tilde{t}} = 500$ GeV) the Wilson coefficient of the dominant operator for the process $b \to s\gamma$, $\mathcal{O}_7$, has the opposite sign in the minimal supersymmetric standard model (MSSM) than for the standard model, i.e. $C_7(\mathrm{MSSM}) \sim -C_7(\mathrm{SM})$ [18]. Recent measurements of the branching ratio $\mathrm{Br}(B \to X_s l^+ l^-)$ [19] suggest that the same sign is preferred, $C_7(\mathrm{MSSM}) \sim C_7(\mathrm{SM})$, while the latest data on the forward-backward asymmetry does not seem to distinguish between these two possibilities [20]. Clearly a more detailed χ^2 analysis including all these processes would be necessary to better test the theory. This is, however, not the focus of the present paper.[12]

In Figs. 3 and 4 we present contours of constant light Higgs mass for the case $m_{16} = 4$ and 5 TeV. There is not much difference in the range of the light Higgs mass in the two cases. We find an upper bound on the Higgs mass given

[12]We have also not calculated $(g-2)_\mu$ in this paper. However, in a previous analysis [5] we found typical values of $(g-2)_\mu < 3 \times 10^{-10}$.

by $m_h \leq 127$ GeV. In our analysis, we use the output of our RG running as input to FEYNHIGGS [21] to obtain the Higgs pole mass at two loops. Note that in the region of parameter space with $|A_0| > m_{16}$, the radiative corrections to the Higgs mass are significant, i.e. the two-loop correction, using FEYNHIGGS, is of order 30 GeV. One might then worry that the theoretical uncertainty in the light Higgs mass is just as big. However, Heinemeyer [22] (see Sec. 2.5) estimates the uncertainties in the light Higgs mass from yet-to-be-calculated two-loop corrections and higher to be at most 3 GeV. We have thus taken ± 3 GeV as the estimated total theoretical uncertainty in the light Higgs mass.[13]

Lepton flavor violation and electric dipole moments

Let us now focus on our results for LFV processes $l_j \to l_i\gamma$ and charged lepton EDMs in this theory. We start with universal squark and slepton masses and a universal A parameter at the GUT scale. This is thus a GUT version of minimal flavor violating boundary conditions, giving minimal flavor violation at low energies. Thus the dominant contribution to lepton flavor violation results from the RG running of slepton masses and the effect of neutrino Yukawa couplings on this running from the GUT scale to the heaviest right-handed neutrino Majorana mass of order 10^{14} GeV. See, for example, the seminal paper on this subject [24]. There is also ample literature regarding LFV and EDMs; see for instance [25,26] for LFV and [27,28] for EDMs. Therefore we simply quote the results of [25,27] here and refer the reader to those references for more detail.

Following the notation of [25], the effective Lagrangian $\mathcal{L}$ relevant for the decay $l_j \to l_i\gamma$ is

$$\mathcal{L} = -\frac{e}{2} m_{l_j} \bar{u}_i \sigma_{\alpha\beta} (A_2^L P_L + A_2^R P_R) u_j F^{\alpha\beta},$$

where e is the electric charge, m_{l_j} is the mass of the decaying lepton, $P_{R/L}$ is the chirality projection operator, and u_i and u_j are Dirac spinors describing l_i and l_j, respectively. $A_2^{L/R}$ is obtained by calculating Feynman diagrams depicted in Fig. 5 at one loop, and found in [25].

The decay amplitude is given by

$$T = ie\epsilon^{\alpha *} m_{l_j} \bar{u}_i (p-q) \sigma_{\alpha\beta} q^\beta (A_2^L P_L + A_2^R P_R) u_j(p),$$

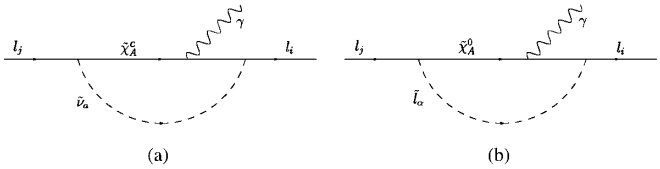

FIG. 5. One-loop Feynman diagrams relevant for the decay of $l_j \to l_i\gamma$. (a) involves charginos $\tilde{\chi}_A^c$ and sneutrinos $\tilde{\nu}_a$, and (b) involves neutralinos $\tilde{\chi}_A^0$ and sleptons $\tilde{l}_\alpha$ in the loop with $A = 1, 2$ for charginos, $A = 1, 2, 3, 4$ for neutralinos, $a = 1, 2, 3$, and $\alpha = 1, \ldots, 6$.

where ϵ^* is the photon polarization vector. Then, the decay rate is

$$\Gamma(l_j \to l_i\gamma) = \frac{e^2}{16\pi} m_{l_j}^5 (|A_2^L|^2 + |A_2^R|^2).$$

On the other hand, the lepton electric dipole moment d_{l_i} is defined as the coefficient of the effective Lagrangian $\mathcal{L}$ of the form

$$\mathcal{L} = -\frac{i}{2} d_{l_i} \bar{u}_i \sigma_{\alpha\beta} \gamma_5 u_i F^{\alpha\beta}.$$

Let us write

$$d_{l_i} \equiv d_{l_i}^{\rm ch} + d_{l_i}^{\rm nt},$$

where $d_{l_i}^{\rm ch}$ and $d_{l_i}^{\rm nt}$ are contributions to the EDM from loops in Figs. 5(a) and 5(b), replacing l_j by l_i, respectively. Then we find

$$d_{l_i}^{\rm ch} = -\frac{e}{16\pi^2} \sum_{A=1}^{2} \sum_{a=1}^{3} {\rm Im}(C_{iAa}^{L(i)} C_{iAa}^{R(i)*}) \frac{m_{\tilde{\chi}_A^+}}{m_{\tilde{\nu}_a}^2} \times \frac{3 - 4x_{Aa} + x_{Aa}^2 + 2\ln x_{Aa}}{2(1-x_{Aa})^3},$$

$$d_{l_i}^{\rm nt} = -\frac{e}{16\pi^2} \sum_{A=1}^{4} \sum_{\alpha=1}^{6} {\rm Im}(N_{iA\alpha}^{L(l)} N_{iA\alpha}^{R(i)*}) \frac{m_{\tilde{\chi}_A^0}}{m_{\tilde{l}_\alpha}^2} \times \frac{1 - x_{A_\alpha}^2 + 2x_{A\alpha}\ln x_{A\alpha}}{2(1-x_{A\alpha})^3}.$$

Here $C_{iAa}^{L(l)}$, $C_{iAa}^{R(l)}$, $N_{iA\alpha}^{L(l)}$, and $N_{iA\alpha}^{R(l)}$ are read from vertices shown in Fig. 6 and the expression for them is given in [25]. $m_{\tilde{\chi}_A^+}$ is the chargino mass, $m_{\tilde{\nu}_a}$ is the sneutrino mass, $m_{\tilde{\chi}_A^0}$ is the neutralino mass, $m_{\tilde{l}_\alpha}$ is the selectron mass, $x_{Aa} \equiv m_{\tilde{\chi}_A^+}^2/m_{\tilde{\nu}_a}^2$, and $x_{A\alpha} \equiv m_{\tilde{\chi}_A^0}^2/m_{\tilde{l}_\alpha}^2$.

Table I shows the current limits on various lepton flavor violating processes and EDMs with an estimated sensitivity for future experiments. See for example [42] for a summary of the current and future experimental status on searches for LFV and the muon EDM.

We note that the MEG Collaboration [30] (searching for $\mu \to e\gamma$ with a sensitivity of order $\geq 5 \times 10^{-14}$) should start taking data by September 2006 and may have signifi-

[13] Our results for the light Higgs mass are about 5 GeV higher than in our previous analyses [4,5]. This is due to the fact that we now use FEYNHIGGS to calculate the Higgs mass, whereas in previous papers we used an effective potential analysis. The disagreement of the effective potential method with FEYNHIGGS (a perturbative analysis) is well known; see for example [23]. In addition, one sees that the light Higgs mass decreases as $M_{1/2}$ increases. This fact is completely due to the global χ^2 analysis and the need to fit the bottom quark mass starting with third family Yukawa unification. For a detailed discussion of this effect, see the second reference in [5].

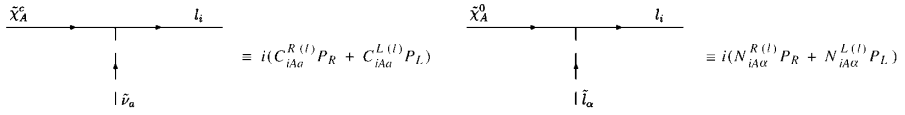

(a) (b)

FIG. 6. Vertices (a) define $C_{iAa}^{L(l)}$ and $C_{iAa}^{R(l)}$ and vertices (b) $N_{iA\alpha}^{L(l)}$ and $N_{iA\alpha}^{R(l)}$ with $A = 1, 2$ for charginos, $A = 1, 2, 3, 4$ for neutralinos, and $\alpha = 1, \ldots, 6$.

cant results by 2008. It will be an excellent test for any new physics beyond the standard model and, in particular, the DR model [1]. Let us also note here that we can calculate $\mathrm{Br}(l_i \to 3l_j)$ to a good approximation by using

$$\frac{\mathrm{Br}(l_i \to 3l_j)}{\mathrm{Br}(l_i \to l_j\gamma)} \simeq \frac{\alpha}{3\pi}\left(\log\frac{m_{l_i^2}}{m_{l_j}^2} - \frac{11}{4}\right),$$

which has been verified in Ref. [43] for all values of $\tan\beta$. In particular,

$$\frac{\mathrm{Br}(\tau \to 3\mu)}{\mathrm{Br}(\tau \to \mu\gamma)} \simeq \frac{1}{440}, \qquad \frac{\mathrm{Br}(\tau \to 3e)}{\mathrm{Br}(\tau \to e\gamma)} \simeq \frac{1}{94},$$
$$\frac{\mathrm{Br}(\mu \to 3e)}{\mathrm{Br}(\mu \to e\gamma)} \simeq \frac{1}{162}.$$

This means that, if we satisfy the constraint from $\mathrm{Br}(l_i \to l_j\gamma)$, we also automatically satisfy the constraint from $\mathrm{Br}(l_i \to 3l_j)$.

In Fig. 7 we plot contours of the constant branching ratio $\mathrm{Br}(\mu \to e\gamma)$ for $m_{16} = 4$ TeV. The prediction is significantly below the present experimental bounds. Moreover, comparing this result with the future sensitivity of the MEG experiment [30] [$\mathrm{Br}(\mu \to e\gamma) > 5 \times 10^{-14}$] we find that our prediction is below the MEG sensitivity in most of the parameter space. Note, however, the narrow region in the upper right hand corner with $\chi^2 \leq 8$ which is within the sensitivity of the MEG experiment. In Fig. 8 we present results for $m_{16} = 5$ TeV. Of course, larger scalar masses suppress the branching ratio, so that now the entire allowed region is below the projected MEG sensitivity. The results for the decays $\tau \to e\gamma$ and $\tau \to \mu\gamma$ are given in Fig. 9. Unfortunately the results are significantly below the present bounds and we are not aware of any experiments to significantly improve these bounds.

We have also evaluated the predictions for the electric dipole moments of the electron, muon, and tau. In Figs. 10 and 11 we present the results for the electric dipole moment of the electron. Note, in both cases, the entire region is below the present bounds, and also within the projected

TABLE I. Current upper limit on various LFV processes and lepton EDMs. The limits on the LFV processes are all at 90% C.L. Estimated accuracy for the future experiment is given for $\mu \to e\gamma$, μe conversion, electron EDM, and muon EDM.

	Current limit	Expected accuracy
$\mathrm{Br}(\mu \to e\gamma)$	$<1.2 \times 10^{-11}$ [29]	5×10^{-14} [30]
$\mathrm{Br}(\tau \to e\gamma)$	$<1.1 \times 10^{-7}$ [31]	...
$\mathrm{Br}(\tau \to \mu\gamma)$	$<6.8 \times 10^{-8}$ [32]	...
$\mathrm{Br}(\mu \to 3e)$	$<1.0 \times 10^{-12}$ [33]	...
$\mathrm{Br}(\tau \to 3l)$	$<1 - 3 \times 10^{-7}$ [34]	...
$\mathrm{Br}(\mu Ti \to eTi)$	$<1.7 \times 10^{-12}$ [35]	10^{-18} [36]
d_e [$e \cdot$ cm]	$<1.6 \times 10^{-27}$ [37]	10^{-31} [38]
d_μ [$e \cdot$ cm]	$<10^{-18}$ [39]	$10^{-24} - 10^{-25}$ [40]
d_τ [$e \cdot$ cm]	$<10^{-16}$ [41]	...

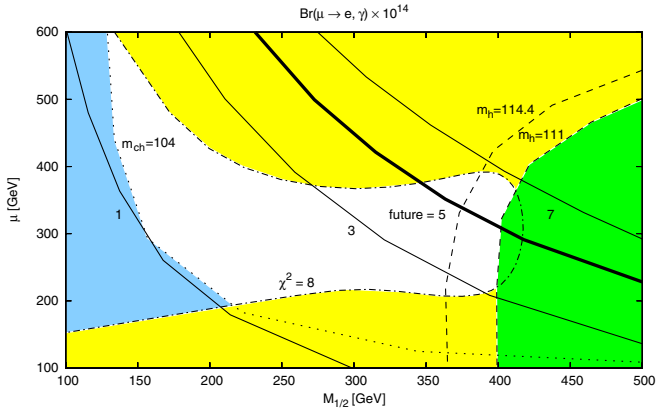

FIG. 7 (color online). Contours of the constant branching ratio $\mathrm{Br}(\mu \to e\gamma) \times 10^{14}$ for $m_{16} = 4$ TeV and $m_A = 700$ GeV. The shaded regions are the same as in Fig. 1. Note the narrow region in the upper right hand corner with $\chi^2 \leq 8$ which is within the sensitivity of the MEG experiment.

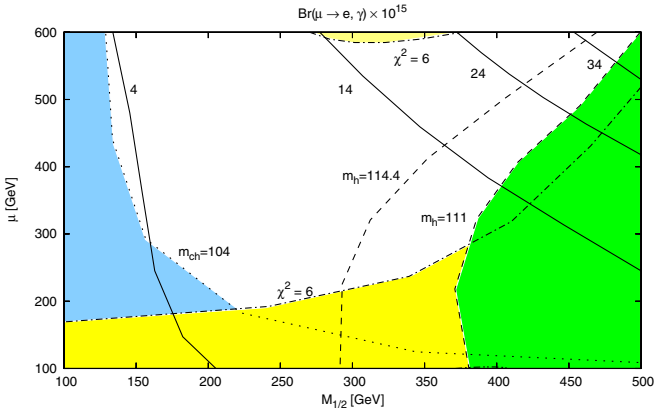

FIG. 8 (color online). Contours of the constant branching ratio $\mathrm{Br}(\mu \to e\gamma) \times 10^{15}$ for $m_{16} = 5$ TeV and $m_A = 700$ GeV. The shaded regions are the same as in Fig. 2. Note all points are below the sensitivity of the MEG experiment.

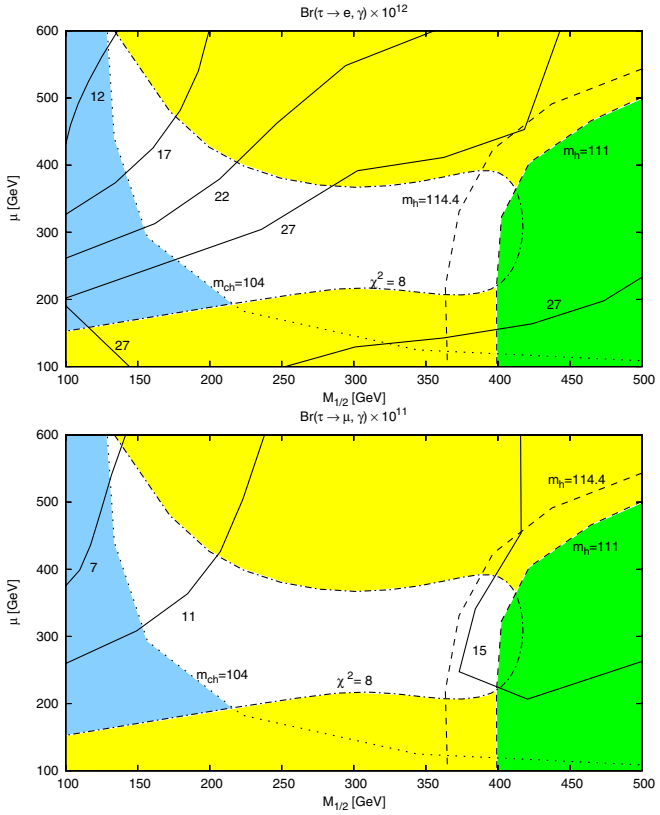

FIG. 9 (color online). Contours of the constant branching ratio $\mathrm{Br}(\tau \to e\gamma) \times 10^{12}$ (upper) and $Br(\tau \to \mu\gamma) \times 10^{11}$ (lower) for $m_{16} = 4$ TeV and $m_A = 700$ GeV. The shaded regions are the same as in Fig. 1.

sensitivity of future experiments [38]. In Fig. 12 we present the results for the electric dipole moments of the muon and tau. In all cases the results are below the present bounds and for d_μ the result is below the projected sensitivity of future experiments [40].

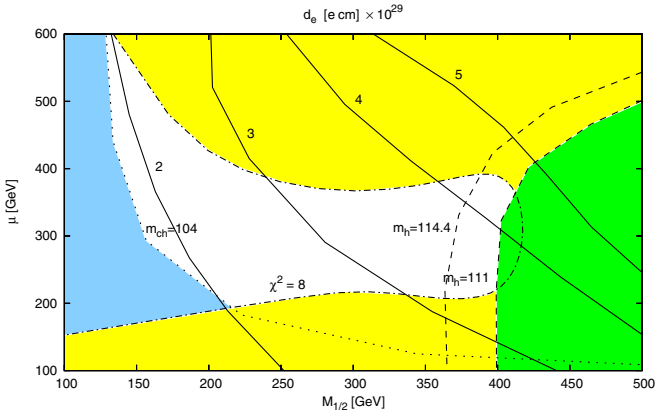

FIG. 10 (color online). Contours of the constant electric dipole moment of the electron, $d_e[e \cdot \mathrm{cm}] \times 10^{29}$, for $m_{16} = 4$ TeV and $m_A = 700$ GeV. The shaded regions are the same as in Fig. 1. Note the entire region is within the sensitivity of future experiments.

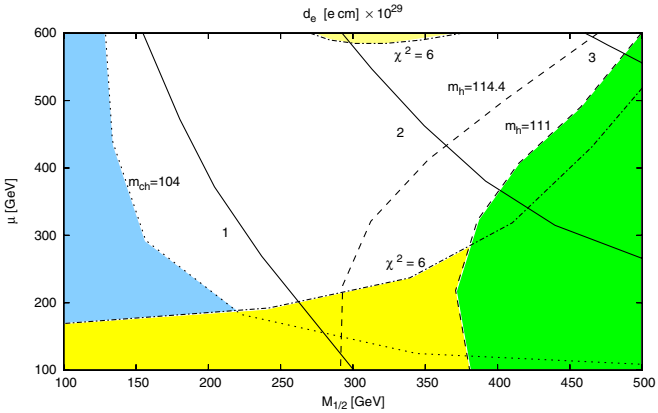

FIG. 11 (color online). Contours of the constant electric dipole moment of the electron, $d_e[e \cdot \mathrm{cm}] \times 10^{29}$, for $m_{16} = 5$ TeV and $m_A = 700$ GeV. The shaded regions are the same as in Fig. 2. Note the entire region is within the sensitivity of future experiments.

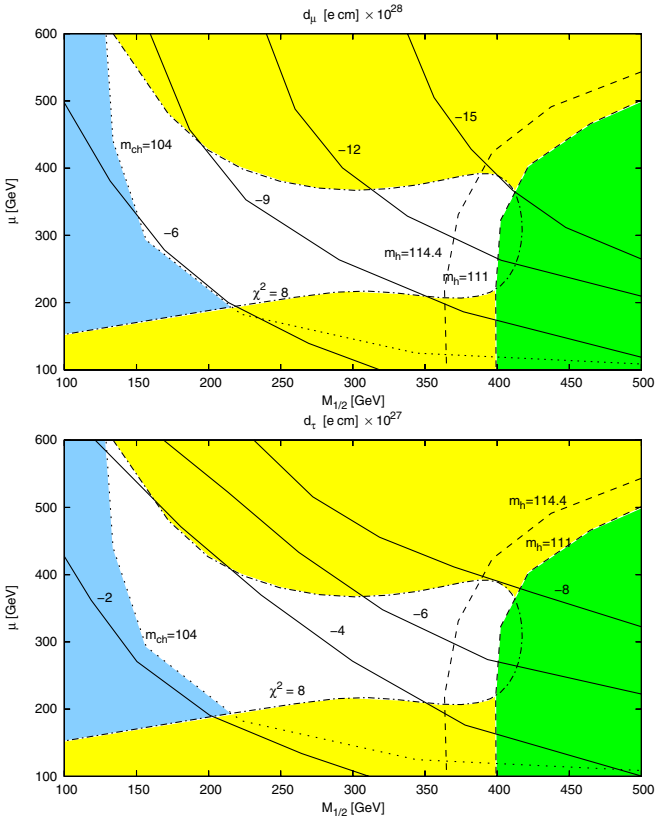

FIG. 12 (color online). Contours of the constant electric dipole moment of the muon, $d_\mu[e \cdot \mathrm{cm}] \times 10^{28}$ (upper), and the tau, $d_\tau[e \cdot \mathrm{cm}] \times 10^{27}$ (lower), for $m_{16} = 4$ TeV and $m_A = 700$ GeV. The shaded regions are the same as in Fig. 1. Note that the entire region is below present bounds and for d_μ the result is below the projected sensitivity of future experiments.

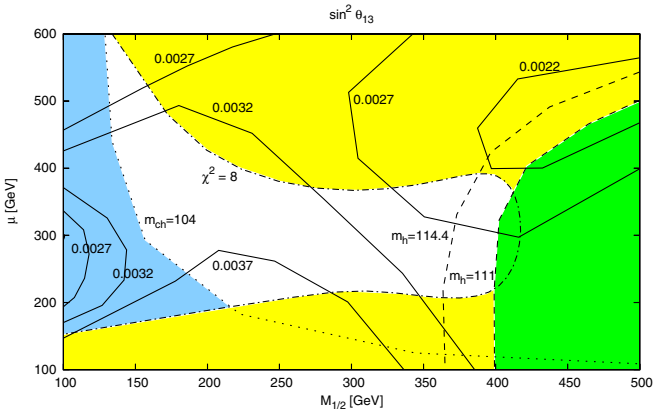

FIG. 13 (color online). Contours of the constant neutrino mixing angle, $\sin^2\theta_{13}$, for $m_{16} = 4$ TeV and $m_A = 700$ GeV. The shaded regions are the same as in Fig. 1.

In Figs. 13 and 14 we evaluate the neutrino mixing angle $\sin^2\theta_{13}$. Recall that measuring this mixing angle is the goal of several future reactor and long baseline neutrino experiments. Moreover, a sufficiently large value for $\sin^2\theta_{13}$ is needed in order to have the possibility of observing *CP* violation in neutrino oscillations. The value of $\sin^2\theta_{13}$ is somewhat sensitive to the value of m_{16}, with a central value changing from $\sin^2\theta_{13} \sim 0.0030 \pm 0.0007$ for $m_{16} = 4$ TeV to $\sin^2\theta_{13} \sim 0.0024 \pm 0.0004$ for $m_{16} = 5$ TeV (where the uncertainty corresponds to varying over the range for μ, $M_{1/2}$ with $\chi^2 \leq 8$ or ≤ 6 in the two cases). Note that, while $\sin^2\theta_{13}$ is relatively insensitive to varying μ, $M_{1/2}$, the *CP* violating parameter $\sin\delta$, on the other hand, is quite sensitive. We find that $\sin\delta$ can vary between 0.1 and 1.0 for different values of μ, $M_{1/2}$, and as a result the *CP* violating Jarlskog parameter J ranges from 0.0013 to 0.013. *CP* violation in the latter case may be observable at long baseline experiments. For example, the J-PARC–SK experiment has a potential sensitivity to $\sin^2 2\theta_{13} <$ 1.5×10^{-3} and $\delta \sim \pm 20°$, and a comparable sensitivity is expected from the "Off-axis NUMI" proposal [44].

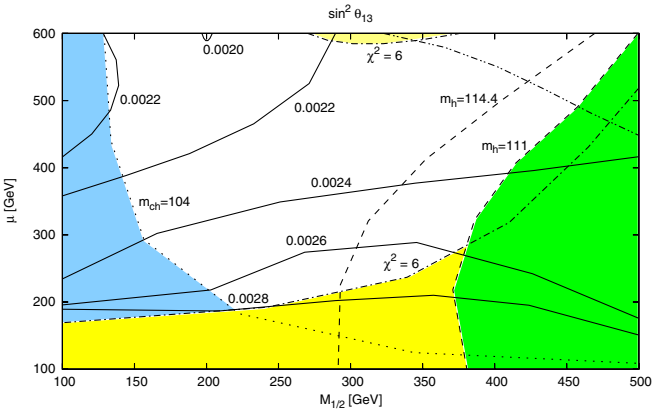

FIG. 14 (color online). Contours of the constant neutrino mixing angle, $\sin^2\theta_{13}$, for $m_{16} = 5$ TeV and $m_A = 700$ GeV. The shaded regions are the same as in Fig. 2.

In Tables II and III we present the χ^2 fit for a particular point in SUSY parameter space for $m_{16} = 4$ and 5 TeV, respectively. The points give a value of $\chi^2 = 7.65$ and 4.99. The former is acceptable while the latter is quite good. In the table captions we present the input data at the GUT scale. We also show the heavy Majorana neutrino masses (roughly 10^{10}, 10^{12}, 10^{14} GeV) responsible for the seesaw mechanism and the light neutrino masses.

Note that the pull from m_b and $M_b - M_c$ is significantly lower for $m_{16} = 5$ TeV than for $m_{16} = 4$ TeV. This accentuates the "tug of war" between the gluino and chargino loop contributions to the bottom quark mass at large $\tan\beta$. The light quark mass ratio m_d/m_s is difficult to fit

TABLE II. The fit for fermion masses and mixing angles at one particular point in SUSY parameter space defined by $m_{16} = 4$ TeV, $\mu = 300$ GeV, and $M_{1/2} = 200$ GeV.

Initial parameters:
$(1/\alpha_G, M_G, \epsilon_3) = (24.84, 3.30 \times 10^{16}\ \text{GeV}, -3.57\%)$
$(\lambda, \epsilon, \sigma, \tilde{\epsilon}, \rho, \epsilon', \xi) =$
$(0.62, 0.030, 0.87, 0.0063, -0.059, -0.0021, 0.0040)$
$(\Phi_\sigma, \Phi_{\tilde{\epsilon}}, \Phi_\rho, \Phi_\xi) = (0.637, 0.453, 0.709, 3.609)$ rad
$(m_{16}, M_{1/2}, A_0, \mu(M_Z)) = (4000, 200, -7809.1, 300)$ GeV
$((m_{H_d}/m_{16})^2, (m_{H_u}/m_{16})^2, \tan\beta) = (1.91, 1.61, 50.34)$
$(M_{R_3}, M_{R_2}, M_{R_1}) = (4.6 \times 10^{13}\ \text{GeV}, 8.1 \times 10^{11}\ \text{GeV}, 1.1 \times 10^{10}\ \text{GeV})$

Observable (mass in GeV)	Data (σ)	Theory	Pull
$G_\mu \times 10^5$	1.166 37 (0.1%)	1.166 38	<0.01
α_{EM}^{-1}	137.036 (0.1%)	137.035	<0.01
$\alpha_s(M_Z)$	0.1187 (0.002)	0.1174	0.37
M_t	172.7 (2.9)	173.11	0.02
$m_b(M_b)$	4.25 (0.25)	4.49	0.94
$M_b - M_c$	3.4 (0.2)	3.61	**1.16**
$m_c(m_c)$	1.2 (0.2)	1.16	0.03
m_s	0.105 (0.025)	0.107	0.01
m_d/m_s	0.0521 (0.0067)	0.0638	**3.09**
$Q^{-2} \times 10^3$	1.934 (0.334)	1.815	0.12
M_τ	1.777 (0.1%)	1.777	<0.01
M_μ	0.105 66 (0.1%)	0.105 66	<0.01
$M_e \times 10^3$	0.511 (0.1%)	0.511	<0.01
V_{us}	0.22 (0.0026)	0.2193	0.06
V_{cb}	0.0413 (0.0015)	0.0410	0.03
V_{ub}	0.003 67 (0.000 47)	0.003 16	**1.15**
V_{td}	0.0082 (0.000 82)	0.008 24	<0.01
ϵ_K	0.002 28 (0.000 228)	0.002 34	0.08
$\sin(2\beta)$	0.687 (0.064)	0.6435	0.46
$\Delta m_{31}^2 \times 10^3$	2.3 (0.6)	2.382	0.01
$\Delta m_{21}^2 \times 10^5$	7.9 (0.6)	7.880	<0.01
$\sin^2\theta_{12}$	0.295 (0.045)	0.289	0.01
$\sin^2\theta_{23}$	0.51 (0.13)	0.532	0.03
Total χ^2			**7.65**

TABLE III. The fit for fermion masses and mixing angles at one particular point in SUSY parameter space defined by $m_{16} = 5$ TeV, $\mu = 300$ GeV, and $M_{1/2} = 200$ GeV.

Initial parameters:
$(1/\alpha_G, M_G, \epsilon_3) = (24.90, 3.29 \times 10^{16}\ \text{GeV}, -3.45\%)$
$(\lambda, \epsilon, \sigma, \tilde{\epsilon}, \rho, \epsilon', \xi) =$
$(0.63, 0.030, 0.77, 0.0070, -0.054, -0.0022, 0.0035)$
$(\Phi_\sigma, \Phi_{\tilde{\epsilon}}, \Phi_\rho, \Phi_\xi) = (0.643, 0.410, 0.692, 3.618)$ rad
$(m_{16}, M_{1/2}, A_0, \mu(M_Z)) = (5000, 200, -9918.9, 300)$ GeV
$((m_{H_d}/m_{16})^2, (m_{H_u}/m_{16})^2, \tan\beta) = (1.91, 1.62, 50.53)$
$(M_{R_3}, M_{R_2}, M_{R_1}) = (6.1 \times 10^{13}\ \text{GeV}, 8.6 \times 10^{11}\ \text{GeV}, 9.6 \times 10^{9}\ \text{GeV})$

Observable (masses in GeV)	Data (σ)	Theory	Pull
$G_\mu \times 10^5$	1.166 37 (0.1%)	1.166 38	<0.01
α_{EM}^{-1}	137.036 (0.1%)	137.036	<0.01
$\alpha_s(M_Z)$	0.1187 (0.002)	0.1178	0.18
M_t	172.7 (2.9)	173.64	0.10
$m_b(M_b)$	4.25 (0.25)	4.49	0.03
$M_b - M_c$	3.4 (0.2)	3.49	0.23
$m_c(m_c)$	1.2 (0.2)	1.08	0.34
m_s	0.105 (0.025)	0.113	0.12
m_d/m_s	0.0521 (0.0067)	0.0629	**2.60**
$Q^{-2} \times 10^3$	1.934 (0.334)	1.824	0.10
M_τ	1.777 (0.1%)	1.777	<0.01
M_μ	0.105 66 (0.1%)	0.105 66	<0.01
$M_e \times 10^3$	0.511 (0.1%)	0.511	<0.01
V_{us}	0.22 (0.0026)	0.2195	0.03
V_{cb}	0.0413 (0.0015)	0.0413	<0.01
V_{ub}	0.003 67 (0.000 47)	0.003 25	0.77
V_{td}	0.0082 (0.000 82)	0.008 12	<0.01
ϵ_K	0.002 28 (0.000 228)	0.002 31	<0.01
$\sin(2\beta)$	0.687 (0.064)	0.6511	0.31
$\Delta m^2_{31} \times 10^3$	2.3 (0.6)	2.408	0.03
$\Delta m^2_{21} \times 10^5$	7.9 (0.6)	7.880	<0.01
$\sin^2\theta_{12}$	0.295 (0.045)	0.288	0.01
$\sin^2\theta_{23}$	0.51 (0.13)	0.537	0.04
Total χ^2			**4.99**

and contributes significantly to the pull in both cases. This mass ratio is particularly sensitive to the Georgi-Jarlskog ansatz relating first and second generation quark and lepton masses. The conflict here is with the very low value of the strange quark mass, of order 105 MeV, preferred by lattice gauge theory calculations. Finally, we note that in a previous analysis [1] $\sin2\beta$ contributed a value of 1.5 to the pull. However, the recent Belle data give a significantly smaller central value for $\sin2\beta$ and now the fit is significantly improved.

We present the additional predictions for squark, slepton, and Higgs masses, at these two points in SUSY parameter space, in Table IV, and for neutrino masses and mixing parameters, in Table V. We have given the value for the effective mass parameter observable in neutrinoless double-beta decay,

$$\langle m_{\beta\beta}\rangle = \left|\sum_i U_{ei}^2 m_{\nu_i}\right| = \left|\sum_i |U_{ei}|^2 m_{\nu_i} e^{i\alpha_i'}\right| \qquad (17)$$

[where $\alpha_i' = \alpha_i + 2\delta$ $(i = 1, 2)$ [45]]. It is predicted to be of order 2×10^{-4} eV which is too low to see in near-future experiments [44,46]. We also give the effective electron-neutrino mass observable, relevant for the analysis of the low energy beta decay of tritium. This mass parameter is

TABLE IV. Predictions for SUSY and Higgs spectra for the fit given in Tables II and III in units of GeV.

Particle	$m_{16} = 5$ TeV	$m_{16} = 4$ TeV
h	120	124
H	699	699
A^0	700	699
H^+	700	701
χ_1^0	81	80
χ_2^0	151	150
χ_1^+	151	150
$\tilde{g}$	605	597
$\tilde{t}_1$	498	496
$\tilde{b}_1$	902	846
$\tilde{\tau}_1$	1686	1421

TABLE V. Predictions for neutrino masses, $\sin^2\theta_{13}$, and CP violation in the lepton sector for the fit given in Tables II and III.

	$m_{16} = 5$ TeV	$m_{16} = 4$ TeV
m_{ν_3} (eV)	0.0492	0.0489
m_{ν_2} (eV)	0.0097	0.0096
m_{ν_1} (eV)	0.0041	0.0036
$\sin^2\theta_{13}$	0.0025	0.0037
J	0.0013	0.013
$\sin\delta$	0.119	0.996
α_1 (rad)	−2.974	−1.771
α_2 (rad)	0.136	1.315
$\langle m_{\beta\beta}\rangle$ (eV)	0.000 10	0.000 38
$m^{\text{eff}}_{\nu_e}$ (eV)	0.0067	0.0067
ϵ_1	0.92×10^{-7}	1.61×10^{-7}

TABLE VI. Predictions for branching ratios for lepton flavor violating processes and the electric dipole moment of leptons for the fit given in Tables II and III.

	$m_{16} = 5$ TeV	$m_{16} = 4$ TeV
$\text{Br}(\mu \to e\gamma)$	4.69×10^{-15}	1.40×10^{-14}
$\text{Br}(\tau \to e\gamma)$	1.26×10^{-12}	2.40×10^{-12}
$\text{Br}(\tau \to \mu\gamma)$	6.13×10^{-11}	1.22×10^{-10}
d_e $[e \cdot \text{cm}]$	9.15×10^{-30}	2.43×10^{-29}
d_μ $[e \cdot \text{cm}]$	-3.58×10^{-28}	-7.93×10^{-28}
d_τ $[e \cdot \text{cm}]$	-1.54×10^{-27}	-2.64×10^{-27}

unaffected by Majorana phases and is predicted to be an order of magnitude larger. The observable

$$m_{\nu_e}^{\rm eff} = \left(\sum_i |U_{ei}|^2 m_{\nu_i}^2\right)^{1/2} \tag{18}$$

is predicted to be of order 6×10^{-3} eV. The current experimental limit is $m_{\nu_e}^{\rm eff} \leq 2.5$ eV with the possibility of future experiments, such as KATRIN, reaching bounds on the order of 0.35 eV [44]. Unfortunately, both mass parameters may be unobservable by presently proposed experiments. Finally, in Table VI, we present the predictions for lepton flavor violation and the electric dipole moments at the same points in SUSY parameter space.

V. SUMMARY AND CONCLUSIONS

In this paper we have performed a global χ^2 analysis on a well-motivated, phenomenologically acceptable, minimal $SO(10)$ SUSY GUT with a D_3 family symmetry. The most stringent constraint comes from assuming Yukawa coupling unification for the third family of quarks and leptons. The χ^2 contours as functions of μ and $M_{1/2}$ for $m_{16} = 4$ and 5 TeV are given in Figs. 1 and 2. We find acceptable solutions with $\chi^2 < 8$ (6) for $m_{16} = 4$ (5) TeV, respectively. We find the light Higgs mass, found using FEYNHIGGS, has an upper bound given by $m_h \leq 127$ GeV (see Figs. 3 and 4). The additional predictions for the SUSY spectrum, and neutrino masses and mixing angles at two particular points in SUSY parameter space are given in Tables IV and V.

In addition to the global χ^2 analysis, we focused on obtaining the rates for several lepton flavor violating processes and also for the charged lepton electric dipole moments. We calculated the branching ratios for the lepton flavor violating processes $\mathrm{Br}(\mu \rightarrow e\gamma)$ (Figs. 7 and 8) and $\tau \rightarrow e\gamma$ and $\tau \rightarrow \mu\gamma$ (Fig. 9). There is only a narrow region in the upper right-hand corner (Fig. 7) with $\chi^2 \leq 8$ which is within the sensitivity of the MEG experiment. We have also evaluated the electric dipole moments of the electron (Figs. 10 and 11) and muon and tau (Fig. 12). In all cases, the results are below the present experimental bounds, and for d_μ the result is below the projected sensitivity of future experiments [40]. However, in both cases, the entire region is within the projected sensitivity of future experiments for d_e [38]. The results for the lepton flavor violating processes and electric dipole moments at the same two particular points in SUSY parameter space are given in Table VI.

ACKNOWLEDGMENTS

M. H. and S. R. are partially supported by the U.S. Department of Energy, Grant No. DOE/ER/01545-868. R. D. is supported by the U.S. Department of Energy, Grant No. DE-FG02-90ER40542. We would like to thank T. Blažek for the use of his code.

[1] R. Dermisek and S. Raby, Phys. Lett. B **622**, 327 (2005).
[2] R. Dermisek and S. Raby, Phys. Rev. D **62**, 015007 (2000).
[3] R. Dermisek, Phys. Rev. D **70**, 073016 (2004).
[4] T. Blazek, R. Dermisek, and S. Raby, Phys. Rev. Lett. **88**, 111804 (2002); Phys. Rev. D **65**, 115004 (2002).
[5] R. Dermisek, S. Raby, L. Roszkowski, and R. Ruiz De Austri, J. High Energy Phys. 04 (2003) 037; R. Dermisek, S. Raby, L. Roszkowski, and R. Ruiz de Austri, J. High Energy Phys. 09 (2005) 029.
[6] V. N. Senoguz and Q. Shafi, Phys. Lett. B **582**, 6 (2004).
[7] T. Blazek, S. Raby, and K. Tobe, Phys. Rev. D **60**, 113001 (1999); **62**, 055001 (2000).
[8] S. Eidelman *et al.* (Particle Data Group Collaboration), Phys. Lett. B **592**, 1 (2004).
[9] S. T. Petcov, New J. Phys. **6**, 109 (2004).
[10] V. Barger, S. L. Glashow, P. Langacker, and D. Marfatia, Phys. Lett. B **540**, 247 (2002).
[11] D. M. Pierce, J. A. Bagger, K. T. Matchev, and R. j. Zhang, Nucl. Phys. **B491**, 3 (1997).
[12] P. H. Chankowski and Z. Pluciennik, Phys. Lett. B **316**, 312 (1993); K. S. Babu, C. N. Leung, and J. T. Pantaleone, Phys. Lett. B **319**, 191 (1993); S. Antusch, J. Kersten, M. Lindner, and M. Ratz, Phys. Lett. B **538**, 87 (2002).
[13] D. Whiteson (CDF Collaboration), hep-ex/0605106.
[14] E. Barberio *et al.* (The Heavy Flavor Averaging Group), hep-ex/0603003.
[15] M. Maltoni, T. Schwetz, M. A. Tortola, and J. W. F. Valle, New J. Phys. **6**, 122 (2004).
[16] R. Dermisek, A. Mafi, and S. Raby, Phys. Rev. D **63**, 035001 (2001).
[17] T. Blazek, M. Carena, S. Raby, and C. E. M. Wagner, Phys. Rev. D **56**, 6919 (1997).
[18] T. Blazek, S. Raby, and S. Pokorski, Phys. Rev. D **52**, 4151 (1995).
[19] P. Gambino, U. Haisch, and M. Misiak, Phys. Rev. Lett. **94**, 061803 (2005); see also A. Ali, E. Lunghi, C. Greub, and G. Hiller, Phys. Rev. D **66**, 034002 (2002); C. Bobeth, A. J. Buras, and T. Ewerth, Nucl. Phys. **B713**, 522 (2005).
[20] A. Ishikawa *et al.*, Phys. Rev. Lett. **96**, 251801 (2006).
[21] S. Heinemeyer, W. Hollik, and G. Weiglein, Comput. Phys. Commun. **124**, 76 (2000); Eur. Phys. J. C **9**, 343 (1999).
[22] S. Heinemeyer, Int. J. Mod. Phys. A **21**, 2659 (2006).
[23] B. C. Allanach, A. Djouadi, J. L. Kneur, W. Porod, and P. Slavich, J. High Energy Phys. 09 (2004) 044.
[24] F. Borzumati and A. Masiero, Phys. Rev. Lett. **57**, 961

(1986).
[25] J. Hisano, T. Moroi, K. Tobe, and M. Yamaguchi, Phys. Rev. D **53**, 2442 (1996).
[26] L. J. Hall, V. A. Kostelecky, and S. Raby, Nucl. Phys. **B267**, 415 (1986); F. Gabbiani, E. Gabrielli, A. Masiero, and L. Silvestrini, Nucl. Phys. **B477**, 321 (1996).
[27] J. R. Ellis, J. Hisano, S. Lola, and M. Raidal, Nucl. Phys. **B621**, 208 (2002); J. R. Ellis, J. Hisano, M. Raidal, and Y. Shimizu, Phys. Lett. B **528**, 86 (2002).
[28] S. Dimopoulos and L. J. Hall, Phys. Lett. B **344**, 185 (1995); S. Abel, S. Khalil, and O. Lebedev, Nucl. Phys. **B606**, 151 (2001).
[29] M. L. Brooks *et al.* (MEGA Collaboration), Phys. Rev. Lett. **83**, 1521 (1999).
[30] M. Grassi (MEG Collaboration), Nucl. Phys. B, Proc. Suppl. **149**, 369 (2005); see also S. Ritt, Report No. PHIPSI06, Novosibirsk, 2006, http://meg.web.psi.ch/docs/.
[31] B. Aubert *et al.* (*BABAR* Collaboration), Phys. Rev. Lett. **96**, 041801 (2006).
[32] B. Aubert *et al.* (*BABAR* Collaboration), Phys. Rev. Lett. **95**, 041802 (2005).
[33] U. Bellgardt *et al.* (SINDRUM Collaboration), Nucl. Phys. **B299**, 1 (1988).
[34] B. Aubert *et al.* (*BABAR* Collaboration), Phys. Rev. Lett. **92**, 121801 (2004).
[35] J. Kaulard *et al.* (SINDRUM II Collaboration), Phys. Lett. B **422**, 334 (1998).
[36] Y. Kuno, Nucl. Phys. B, Proc. Suppl. **149**, 376 (2005); J-PARC Letter of Intent L25.
[37] B. C. Regan, E. D. Commins, C. J. Schmidt, and D. DeMille, Phys. Rev. Lett. **88**, 071805 (2002).
[38] D. Kawall, F. Bay, S. Bickman, Y. Jiang, and D. DeMille, AIP Conf. Proc. **698**, 192 (2004).
[39] J. Bailey *et al.* (CERN-Mainz-Daresbury Collaboration), Nucl. Phys. **B150**, 1 (1979).
[40] F. J. M. Farley *et al.*, Phys. Rev. Lett. **93**, 052001 (2004); J. P. Miller *et al.* (EDM Collaboration), AIP Conf. Proc. **698**, 196 (2004); B. Lee Roberts, Nucl. Phys. B, Proc. Suppl. **147**, 69 (2005); J. P. Miller, Nucl. Phys. B, Proc. Suppl. **149**, 386 (2005); J-PARC Letter of Intent L22.
[41] K. Inami *et al.* (Belle Collaboration), Phys. Lett. B **551**, 16 (2003).
[42] M. Aoki, Nucl. Phys. B, Proc. Suppl. **143**, 64 (2005); M. Grassi, Nucl. Phys. B, Proc. Suppl. **147**, 61 (2005); B. L. Roberts, M. Grassi, and A. Sato, hep-ex/0510055; also see B. E. Sauer, in Proceedings of the Lepton Moments International Symposium, Cape Cod, MA, 2003, http://g2pc1.bu.edu/leptonmom/talks/Sauer.pdf; D. DeMille, in Proceedings of the Lepton Moments International Symposium, Cape Cod, MA, 2003, http://g2pc1.bu.edu/leptonmom/talks/demille.pdf; S. K. Lamoreaux, Phys. Rev. A **66**, 022109 (2002); J. M. Amini, C. T. Munger, and H. Gould, physics/0602011.
[43] E. Arganda and M. J. Herrero, Phys. Rev. D **73**, 055003 (2006).
[44] R. D. McKeown and P. Vogel, Phys. Rep. **394**, 315 (2004).
[45] S. M. Bilenky, S. Pascoli, and S. T. Petcov, Phys. Rev. D **64**, 053010 (2001).
[46] S. Pascoli and S. T. Petcov, Phys. Lett. B **580**, 280 (2004).